Nonlinear Synchronized LC Oscillators: Theory and Simulation

Michal Odyniec

Abstract—**The paper presents a rigorous analysis of synchronized oscillators. The analyzed circuits exhibit strongly nonlinear behavior such as frequency lock and existence of multiple solutions and yet their behavior can be fully determined by large signal characteristics obtained from harmonic balance simulation. The results can be directly applied to diode and transistor oscillators and can also serve as a benchmark in testing nonlinear simulators.**

I. Introduction

THE PAPER presents simulation and theory of a synchronized nonlinear oscillator. It is based on the theory of averaging [1], [2], presented in terms familiar to a design engineer and illustrated by a transistor oscillator circuit.

We intend to achieve three goals:

1. Introduce a simple yet rigorous[1] analysis of synchronization in typical oscillators.

2. Present applications of harmonic balance simulation to a strongly nonlinear circuit. In particular we present a simple algorithm for finding oscillations and stability zones.

3. Present a benchmark against which nonlinear simulators can be tested.

We show that if a high-Q oscillator has a N-shaped nonlinear characteristics, then one can rigorously deduce important design features of the circuit, such as the number of solutions and their stability, nonlinear resonance characteristics and lock-in regions, and also the parameter values for which the unique solution exists. The results are formulated in terms of "large signal" characteristics and are readily applicable to diode and transistor oscillators.

In the final section of the paper the synchronized oscillator is used as a benchmark against which different commercially available nonlinear simulators can be tested. We believe that there is a great need for such a benchmark in the engineering community. Our circuit seems to be ideally suited for this purpose: it is very simple, and yet it models frequency lock, possesses multiple solutions, and has interesting resonance characteristics which bend onto themselves (that poses an additional challenge for CAD packages—namely the ability to draw the multivalued characteristics). Moreover for the special case of the circuit (described by the van der Pol oscillator) the characteristics are well known and can be used to check accuracy of CAD simulators.

Manuscript received November 18, 1991; revised September 14, 1992.

The author is with Hewlett-Packard Co., Santa Rosa Systems Division, Santa Rosa, CA 95403.

IEEE Log Number 9207423.

[1] By "rigorous" we mean an analysis supported by analytically proven theorems; so that when we find approximate solutions using a harmonic balance simulator, we are sure that the exact solutions exist, are close to the approximate ones, and have the same stability properties.

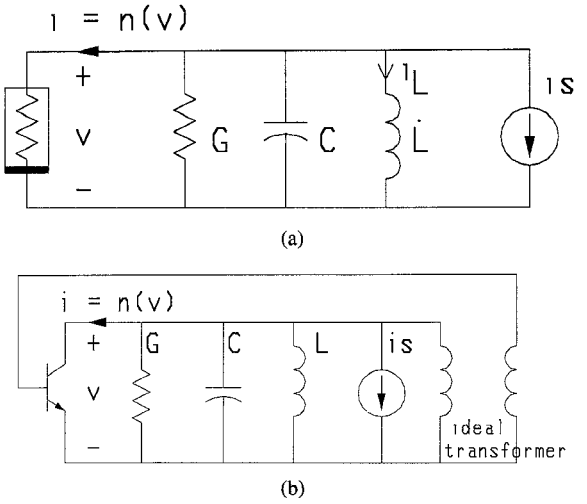

Fig. 1. Oscillator with the locking signal $i_s = b\cos\omega t$ (a) Generic oscillator model. (b) Meissner oscillator.

II. Circuit Description

2.a Generic RLC Oscillator with Synchronizing Signal

Let us consider a simple oscillator with locking signal $i_s = b\cos\omega t$, shown in Fig. 1a, in which the resonator is modelled by a parallel RLC circuit and the active part of the circuit by an N-shaped nonlinear characteristic:

$$i = n(v)$$

where $n'(0)$ can be interpreted as the small signal conductance of the active part of the circuit.

The circuit is described by a simple second other equation:

$$\begin{aligned} L\frac{di_L}{dt} &= v \\ C\frac{dv}{dt} &= -i_L - n(v) \\ &\quad - Gv - b\cos\omega t \end{aligned} \tag{1}$$

Note that we assume very little about the nonlinear characteristics which makes our results easily applicable to wide class of oscillators. Thus the equations (1) apply directly to the circuits in which current-voltage characteristics are N-shaped. This includes IMPATT, Gunn, and tunnel diode oscillators, also Meissner oscillator shown in Fig. 1(b).

One can further argue that various resonators are (at least about the resonace) well modelled by an RLC resonator, and that transistors with feedback, and of course negative-resistance diodes, have the N -shaped characteristics. Therefore the circuit of Fig. 1(a) can be treated as a generic oscillator, which possesses the main features of any high-Q oscilator circuit.

Throughout the paper we shall use two examples: (i) Meissner oscillator (Fig. 1(b)) to illustrate design applications and (ii) van der Pol oscillator (Fig. 1(a)) with $n(v) = -v + v^3/3, G = 0$) for connection to well-established theory.

2.2 Simplified Circuit Equations

When the circuit has high Q and we expect the oscillations to be close to sinusoidal, then it is convenient to introduce amplitude and phase (a, ϕ) as the new variables defined by:

$$v(t) = a\cos(\omega t + \phi) \qquad i_L(t) = a\frac{\sin(\omega t + \phi)}{\omega L} \tag{2}$$

and to work with the following "averaged"[2] equations:

$$a' = -\frac{Ga + N(a) + b\cos(\phi)}{2C} \tag{3}$$

$$\phi' = -\frac{\delta}{2C} + \frac{b\sin(\phi)}{2Ca} \tag{4}$$

where (a, ϕ) denote the amplitude and phase of oscillations, b denotes the amplitude and ω the frequency of the locking signal, $\omega_0^2 = 1/LC$ the natural frequency, $\delta = C(\omega^2 - \omega_0^2/\omega) \approx 2C(\omega - \omega_0)$ "the amount of detuning," and

$$N(a) = \frac{2}{\pi}\int_0^{\pi} n(a\cos\theta)\cos\theta\, d\theta \tag{5}$$

denotes the fundamental of the current. We show in the next section that $N(a)$ can be easily obtained from harmonic balance simulators.

One proves [1, 2] that for high-Q oscillators the amplitude and phase of oscillations are well approximated by the constant solutions of (3) and (4) and that if the constant solutions are stable so are the oscillations. Let us note that the constant solutions of the averaged equations coincide with those obtained by the harmonic balance method [3], [5], [8].

2.3 Nonlinear RF Characteristics $N(a)$

The nonlinear RF characteristics $N(a)$, defined above, is the fundamental component of Fourier expansion of the current through the nonlinear element and has the physical meaning of "large-signal amplitude," similar to phasors used in linear analysis. It can be used to define "large signal" impedance and "large signal" S-parameters [7], [9].[3] It is the basic tool in nonlinear design. When expressed in terms of S-parameters it has been applied to design of free running oscillators in [6], [7], [9], [12].

[2]The detailed transformation of (1) into (3)–(4) is presented in Appendix II.

[3]Where the phasors used in the standard definition are replaced by the fundamental. Let us also note that the S-parameters as measured on a vector analyzer are indeed the ratios of fundamentals of the incident and reflected signal.

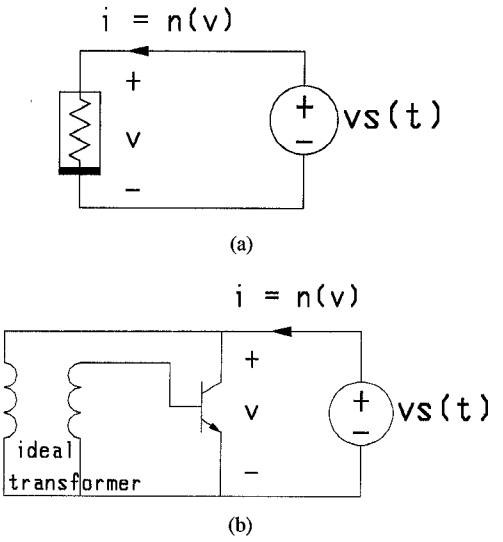

Fig. 2. Simulation of the large signal characteristics $N(a)$, $vs(t) = a\cos\omega t$. (a) Generic oscillator, (b) Meissner oscillator.

In this paper, $N(a)$ and $N'(a)$ (which is the derivative of $N(a)$ with respect to a) become the main vehicle in applying the theoretical results on averaging to the characteristics obtained from the harmonic balance simulation.

They are calculated as follows: In the oscillator circuit we put the locking signal equal to zero and replace the resonator by a sinusoidal voltage source as shown in the Fig. 2(a) and (b) (in our example the parallel resonator is replaced by a voltage source, a series resonator would be replaced by a current source). Then we use the harmonic balance simulator to sweep the source amplitude a and to find the fundamental component of the current which equals to $N(a)$ defined by the formula (5). Some harmonic balance simulators, such as the HP Microwave Design System used here, allow the user to calculate derivatives of the circuit variables with respect to circuit parameters and other circuit variables. We use this capability to calculate $N'(a)$—the derivative of the current fundamental $N(a)$ with respect to the swept amplitude.

2.3.1 Example 1: $N(a)$ and $N'(a)$ simulated in the way described above are shown in Fig. 3 for Meissner oscillator at two bias points.

2.3.2 Example 2: $N(a)$ and $N'(a)$ simulated in the way described above are shown in Fig. 4 for van der Pol cubic nonlinearity (Fig. 1(a) with $n(v) = -v + v^3/3, G = 0$). In this case they can be also found analytically (see (40) in Appendix II, Section B), the plots simulated for the circuit in Fig. 2(a) and the ones calculated from the equation (40) are shown in Fig. 4(b), their traces are the same and cover each other.

III. Synchronized Oscillations

We show in this section how the large signal characteristic $N(a)$ can be used to determine the existence and stability of synchronized oscillations. For sake of clarity we shall use $N(a)$ simulated for the Meissner oscillator (Fig. 1(b)), biased at point $Q1$ (Fig. 3(b)), however, the analysis remains valid for any high-Q circuit with N-shaped nonlinear characteristics.

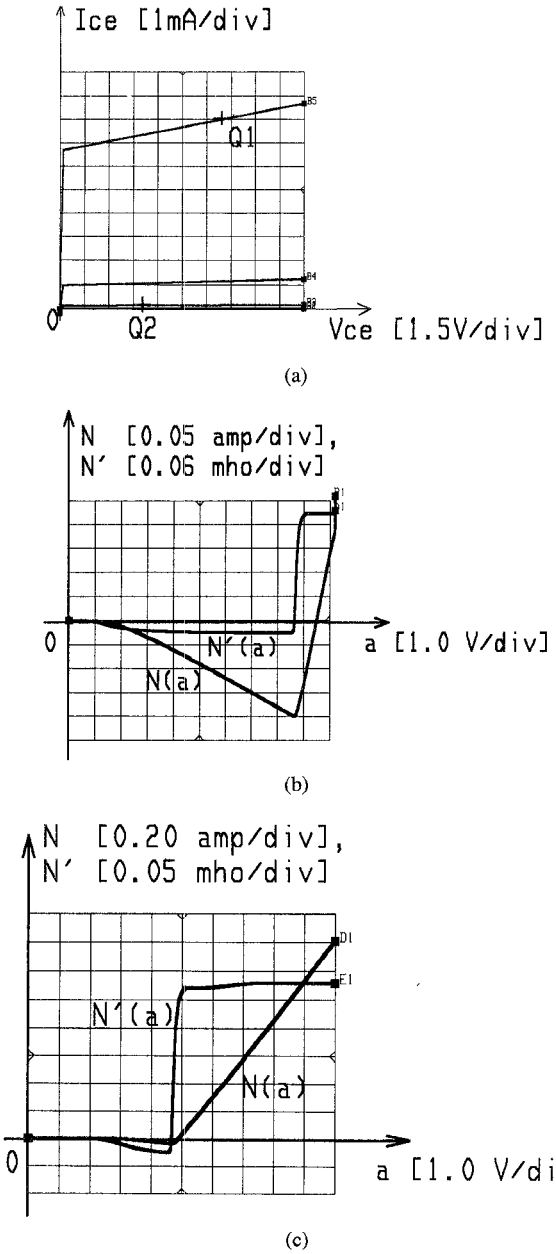

Fig. 3. Large signal characteristics $N(a)$ for Meissner oscillator at different bias. (a) operating points, (b) $N(a)$ for bias at $Q1$, (c) $N(a)$ for bias at $Q2$.

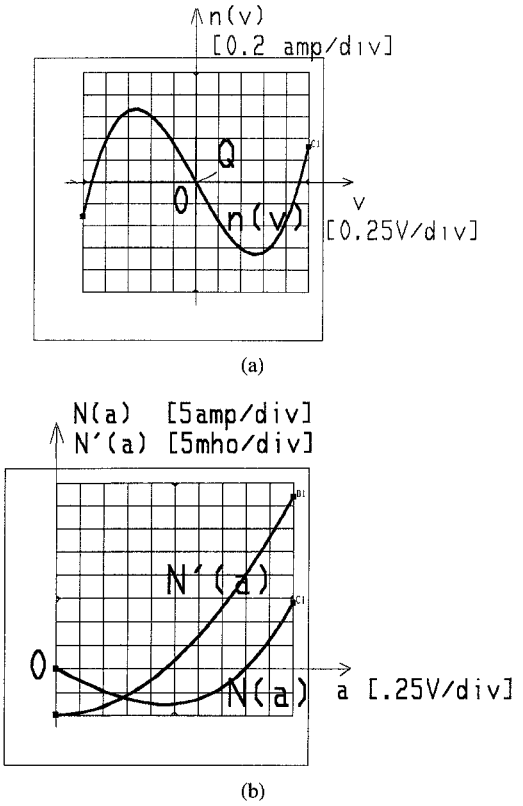

Fig. 4. Van der Pol oscillator, (a) current-voltage characteristics $n(v)$. (b) The simulated large signal characteristics $N(a)$ and its derivative $N'(a)$ coincide with those calculated analytically.

3.1 Resonance Characteristics

In this section we derive a simple algebraic equation, which describes the relationship between the amplitude of the oscillations a and that of the locking signal b and the amount of detuning δ. Moreover, for fixed detuning or fixed forcing, the equation can be easily represented graphically.

Let us note that a constant solution of the equations (3) and (4) can be found from:

$$Ga + N(a) = -b\cos\phi \qquad \delta a = b\sin\phi \tag{6}$$

Consequently the constant solution exists only if the following inequality holds:

$$\delta < \frac{b}{a} \tag{7}$$

This condition is a rigorous representation of the fact that the frequency locks only when the synchronizing frequency is close to the natural frequency of the circuit (i.e., the "amount of detuning" is small).

Adding up the squared sides of (6) we conlcude that the amplitude of locked oscillations satisfies the scalar equation:

$$(Ga + N(a))^2 + a^2\delta^2 = b^2 \tag{8}$$

The above equation describes the relationship between the oscillations amplitude a, the forcing amplitude b, and the forcing frequency (represented here by detuning δ). Let us interpret the equation (8) graphically for (i) fixed δ and (ii) fixed b: (i) fixed detuning δ (Fig. 5(a)).

Since we have already simulated the $N(a)$, we can easily plot the left hand side of (8) (denoted lhs in the Fig. 5(a)) for different values of detuning δ. Consider for example the $N(a)$ simulated for the Meissner oscillator at the operating point $Q1$ (see Fig. 3(b)). The left hand side of (8), obtained for different values of detuning $\delta = 0.0, 0.02, 0.04, 0.07$, and for $N(a)$ from the Fig. 3(b) are shown in the Fig. 5(a). From those plots we can determine graphically the solutions of (8), i.e., the amplitudes of synchronized oscillations. Indeed, for any value of b we find the value a for which a trace shown in the Fig. 5(a) equals b^2, the amplitude a found in this way is the solution of (8).

For instance let $b = 0.2\,(b^2 = 0.04)$. From Fig. 5(a) we can find the amplitude of oscillations for different amounts of

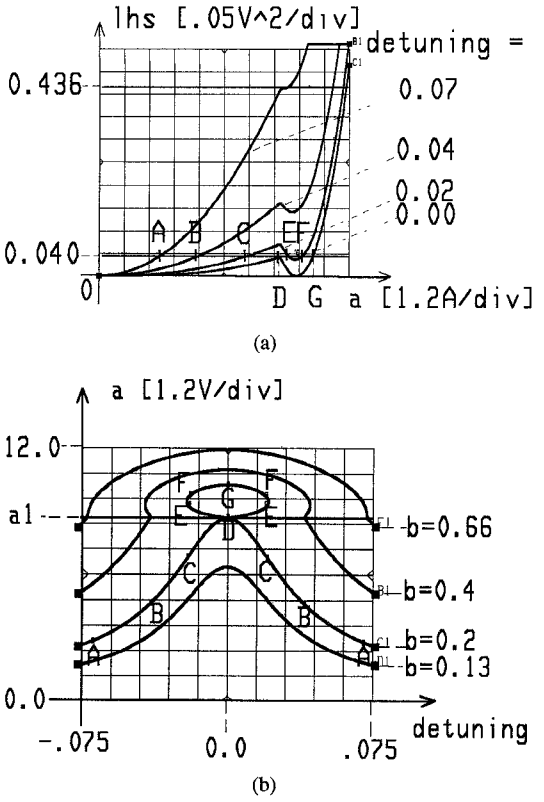

Fig. 5. Graphical representation of (8) for Meissner oscillator biased at point $Q1$. A, B, C, D, E, F, G denote the solutions obtained for $b = 0.2$ and $\delta = 0.07, 0.04, 0.02, 0.0$. (a) The curved traces correspond to the left hand side of the equation (8), simulated for different δ. The horizontal lines denote different levels of the square of the synchronizing amplitude b; if $b^2 > 0.436$ (i.e. $b > 0.66$) we get a unique solution, if $b < 0.66$ we get three solutions, if $b^2 < 0.04$ (i.e. $b < 0.2$), then the frequency characteristics (shown in Fig. 5(b)) becomes disconnected. (b) Resonance characteristics (amplitude vs. detuning). Different traces correspond to different amplitudes of the synchronizing signal: $b = 0.13, 0.2, 0.4, 0.66$.

detuning. For $\delta = 0.07 mho$[4] the oscillations amplitude equals 2.8 V (point A in Fig. 5(a)), for $\delta = 0.04 mho$ it equals 4.5 V (point B in Fig. 5(a)), for $\delta = 0.02 mho$ we get 3 solutions with amplitudes equal to 6.8 V, 9.2 V, and 9.7 V (points C, E, and F in Fig. 5(a)), for $\delta = 0.00 mho$ we get 2 solutions with amplitudes equal to 8.6 V and 10.2 V (points D and G in Fig. 5).

This procedure can be repeated for any b and δ.

Even greater advantage of the plots shown in the Fig. 5(a) is that using them one can easily determine the region in which the multiple solutions exist. Let us note that, because of the N-shaped nonlinear characteristics, the plots bend for small amounts of detuning $\delta < .07$ and become monotonic for large ones, when δa dominates the decreasing part of $N(a)$ in (8).

Therefore if $b < 0.66$ and $\delta < 0.7$, then the system possesses 3 solutions (this is the region where the curves bent), otherwise only one solution exists (either curves in Fig. 5(a) are monotonic or b crosses them above the bent part). (ii) Fixed forcing b.

Alternatively the behavior of the circuit can be (and indeed is most often) represented by the resonance characteristics which represent variation of amplitude of oscillations versus detuning i.e., a vs δ. Fig. 5(b) shows those characteristics, simulated for Meissner oscillator, for the forcing equal to $b = 0.13, 0.20, 0.40, 0.66$.

Note that the specific "inverted vase" or "octopus" shape, which is a typical feature of those plots, is the immediate consequence of the property that the nonlinear characteristics $n(v)$ is N-shaped.

Similarly as before we can find the amplitude of oscillations. For instance if we take the characteristic for $b = 0.2$ we easily find amplitudes for any value of detuning, in particular for $\delta = 0.07, 0.04, 0.02, 0.0$, we get the same amplitudes ($a = 2.8, 4.5, 6.8, 8.6, 9.2, 9.7, 10.2$) as in the Fig. 5(a), marked here by A, B, C, D, E, F, G.

As before the regions in which multiple solutions exist are easy to determine: the answer is the same as above: $\delta < .07, b < 0.66$.

To this author's knowledge the resonance characteristics have been presented in the past only for the van der Pol oscillator [3], [4], [10], [11]. Here we have shown how to apply them to general circuits.

3.2 Synchronization Zones

In the previous section we have determined conditions of existence and the number of steady state oscillations and behavior of their amplitude as a function of detuning. However, in order to analyze the frequency lock we need to determine their stability. For that purpose we use the characteristic $N(a)$ and its derivative $N'(a)$ determined above.

We prove here that the stable oscillations correspond to those parts of resonance characteristics which lie above a certain critical number a_1 and decrease when $|\delta|$ grows.

Let us return to the circuit equations (3) and (4) and calculate the trace and the determinant of their Jacobian matrix:

$$tr(a) = -\frac{1}{2C}\left(2G + N'(a) + \frac{N(a)}{a}\right) \tag{9}$$

$$\Delta(a) = \frac{1}{4C^2}((G + N'(a))\left(G + \frac{N(a)}{a}\right) + \delta^2\right) \tag{10}$$

which can be calculated by a harmonic balance simulator with ability to use equations, such as the HP Microwave Design System used here.

We show in Appendix I that the stability of the solutions of (3) and (4) can be determined from the plots of $tr(a)$ and $\Delta(a)$. We also prove in Appendix I that for an "N -shaped" $n(v)$, there exists a critical value $a1$ (see Fig. 5(b) and Fig. 6) such that the stable oscillations correspond to those parts of resonance characteristics which lie above $a1$ and decrease when $|\delta|$ grows.

We can now formulate the algorithm for finding the synchronization zones:

Algorithm:

0. Put the synchronizing signal to zero and replace the reasonator by a sinusoidal source.

1. Perform harmonic balance simulation sweeping the amplitude of the introduced source.

[4] since we included capacitance in the definition of detuning in (3) and (4) its unit became a "mho."

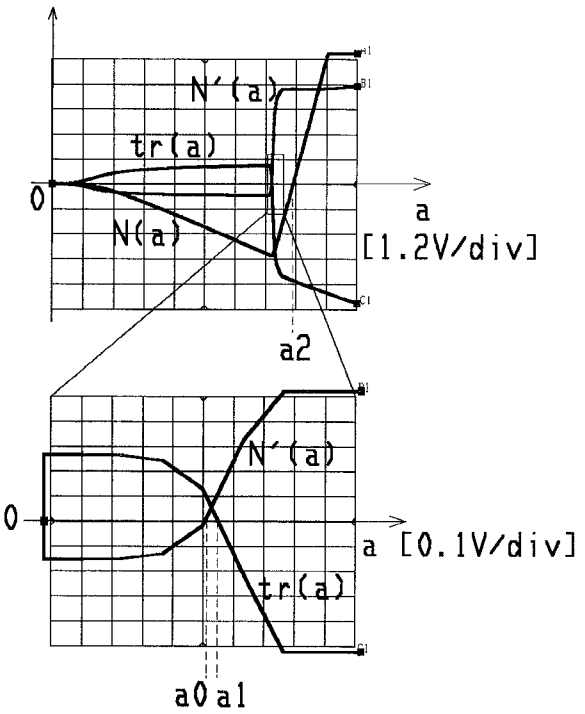

Fig. 6. Plots of $N(a), N'(a)$, and $tr(a)$ simulated for the Meissner oscillator biased at point $Q1$. The values of a at which $N(a), N'(a)$, and $tr(a)$ cross zero are marked respectively as a_2, a_0, a_1.

2. Plot the resonance characteristics i.e., the oscillations amplitude vs. detuning.

3. Plot $tr(a)$, determine a_1.

4. For any detuning and forcing find the amplitude of oscilations as shown in the Fig. 5(b). If a resonance characteristic bends over itself, then the circuit has three solutions, the stable solution corresponds to those parts of resonance characteristics which lie above $a1$ and decrease when $|\delta|$ grows. For the large forcing the characteristics do not bend and the unique solution is stable as long as the oscillations amplitude remains larger than $a1$.

3.2.1 Example 1 Concluded

Let us return to the Meissner oscillator biased at point $Q1$:

The resonance characteristics obtained for different amplitudes of the synchronizing signal are shown in the Fig. 5(b), the plot of $tr(a)$ is shown in Fig. 6.

From the Fig. 6 we find $a1$ and plot it in the Fig. 5(b). The part of the single valued characteristics "$b = .66$" which lie above $a1$, and the parts of the multivalued characteristics "$b = .4, b = .2$" limited by vertical slopes correspond to stable oscillations.[5]

It follows from the Fig. 5(a) that for small values of synchronizing signal (such that $b^2 < .04$) the resonance characteristics become disconnected. One part of such a disconnected characteristic, obtained for $b = .13$, appears in the Fig. 5(b). The other part which is not shown there can be found from the Fig. 5(a).

[5]The characteristic $b = 0.4$ has yet another stability region: when the characteristic bends the second time there is a small region when it still remains above a_1 and decreases with growing $|\delta|$, the region corresponds to stable oscillations.

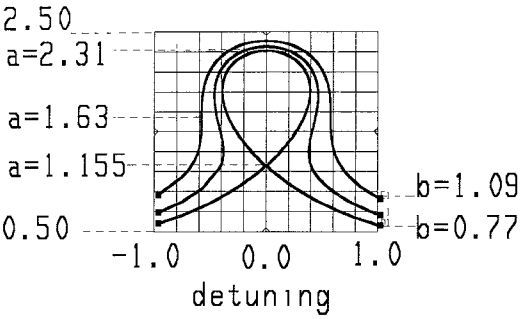

Fig. 7. Resonance characteristics for van der Pol oscillator.

IV. Van der Pol Oscillator as a Benchmark

In this section we use the van der Pol oscillator to check accuracy of a commercially available CAD package.

In the case analyzed by van der Pol $(n(v) = -v + (v^3/3), G = 0, C = 1F, L = 1H)$ we can explicitly find $N(a), N'(a)$:

$$N(a) = -a\left(1 = \left(\frac{a}{2}\right)^2\right) \tag{11}$$

$$N'(a) = -1 - 3\left(\frac{a}{2}\right)^2 \tag{12}$$

Consequently, in order to check accuracy of a CAD package, one can compare the simulated characteristics and the ones calculated analytically as shown in the Fig. 4(b) above.

We can also calculate explicitly (8)

$$a^2\left(\left(1 - \left(\frac{a}{2}\right)^2\right)^2 + \delta^2\right) = b^2 \tag{13}$$

and use it to check accuracy of the simulated resonance characteristics. For example we can find from (13) that the smallest value for which the resonance characteristics do not split is $b = 0.77$ A (which is the value of local maximum of the left hand side of (13) for $\delta = 0$). In that case $(b = 0.77, \delta = 0)$ the amplitude of oscillations equal to $a = 1.155$ V and $a = 2.309$ V. Similarily the minimum value of b for which there are no multiple solutions is $b = 1.09$ A and the corresponding amplitude and detuning (i.e., the smallest detuning at which there are no multiple solutions) are $a = 1.63, \delta = 0.577$ (which is the value of δ at which the left hand side of (13) ceases of have local maximum).

As shown in Fig 7, the simulated results coincide with those calculated above.

V. Conclusions

We have presented simulation and theory of synchronized nonlinear oscillators. Throughout the paper we heavily relied on harmonic balance simulation and showed how its results could be enhaneed by the theory of averaging.

We used HP Microwave Design System to obtain the large-signal characteristic $N(a)$ and resonance characteristics for Meissner oscillator, to the author's knowledge such characteristics were obtained in the past only for van der Pol oscillator.

Those characteristics allowed us to determine the oscillations stability and the areas where multiple solutions exist and also to determine the oscillations amplitude for a given b and δ (i.e., the amplitude and frequency of the synchronizing signal).

Finally we provided explicit formulae against which any simulator can be easily tested.

APPENDIX I

STABILITY

A. Averaged Equations

The stability of constant solutions of (3) and (4) can be determined by the sign of the trace tr and determinant Δ of the right hand side linearized about these solutions.

Namely, the solution is stable if $\Delta > 0$ and $tr < 0$. It turns out that both the determinant and the trace can be determined by $N(a)$ and its derivative. Since both $N(a)$ and $N'(a)$ can be simulated and plotted we are able to determine stability of oscillations from the nonlinear resonance characteristics.

Indeed the averaged equation reads:

$$a' = -\frac{Ga + N(a) + b\cos\phi}{2C} \tag{14}$$

$$\phi' = -\frac{\delta}{2C} + \frac{b\sin\phi}{2Ca} \tag{15}$$

its Jacobian matrix (derivative) equals to

$$J = \begin{bmatrix} -\frac{G}{2C} - \frac{N'(a)}{2C} & +\frac{b\sin\phi}{2C} \\ -\frac{b\sin\phi}{2Ca^2} & \frac{b\cos\phi}{2Ca} \end{bmatrix}$$

As it is evaluated at the constant solution at which:

$$Ga + N(a) = -b\cos\phi \tag{16}$$

$$\delta a = b\sin\phi \tag{17}$$

we get:

$$J = \frac{1}{2C}\begin{bmatrix} -(G + N'(a) & \delta a \\ -\delta/a & -\left(G + \frac{N(a)}{a}\right) \end{bmatrix}$$

and consequently:

$$tr(a) = -\frac{1}{2C}\left(2G + N'(a) + \frac{N(a)}{a}\right) \tag{18}$$

$$\Delta(a) = \frac{1}{4C^2}\left((G + N'(a))\left(G + \frac{N(a)}{a}\right) + \delta^2\right) \tag{19}$$

To simplify notation let us define:

$$\tilde{N}(a) = Ga + N(a) \tag{20}$$

so that:

$$tr(a) = -\frac{1}{2C}\left(\tilde{N}'(a) + \frac{\tilde{N}(a)}{a}\right) \tag{21}$$

$$\Delta(a) = \frac{1}{4C^2}\left(\tilde{N}'(a)\left(\frac{\tilde{N}(a)}{a}\right) + \delta^2\right) \tag{22}$$

Once we have got the above formulae we can determine stability of oscillations by plotting $tr(a)$ and $\Delta(a)$.

B. Stability

For the N-shaped nonlinear characteristics stability becomes very easy to determine. Namely as oscillation's stability is determined by the signs of tr and Δ we shall present geometrical criteria for evaluation of their signs.

Let us start with the trace tr, a typical function $\tilde{N}(a)$ is negative for small a and monotonically decreases till some value which we denote a_0, it then increases until it reaches zero at a_2 and remains growing and positive (see Fig. 6). Consequently $\tilde{N}'(a)$ is negative for $a < a_0$ and positive for $a > a_0$. Therefore the trace is always positive for $a < a_0$ and negative for $a > a_2 \geq a_0$. The only area where the sign of $tr(a)$ is in doubt is between a_0 and a_2 where $\tilde{N}(a)$ is negative and $\tilde{N}'(a)$ positive, but because both functions grow monotonically[6] for $a_0 \leq a \leq a_2$ there is exactly one value a_1 such that the trace equals zero $a = a_1$ and is negative for $a > a_1$. Therefore the trace is negative on those parts of resonance characteristics which lie above a_1.

To determine stability for $a > a1$ we need to check Δ, we prove below that its sign is directly related to the slope of resonance characteristics (such as shown in Fig. 5).

Lemma: For $\Delta > 0$ the resonance characteristics decrease when $|\delta|$ grows, for $\Delta < 0$ they increase when $|\delta|$ grows, for $\Delta = 0$ they become vertical.

Therefore the stable oscillations correspond to those parts of resonance characteristics which lie above a_1 and decreases when $|\delta|$ grows.

Proof of the Lemma:

Note that in terms of $\tilde{N}(a)$ equation (8) takes the form:

$$(\tilde{N}(a))^2 + (\delta a)^2 = b^2 \tag{23}$$

We show that the sign of Δ can be determined from resonance characteristics; namely Δ is positive on those parts of resonance characteristics which decrease when the amount of detuning $|\delta|$ grows. For sake of being specific let us consider the case when $\delta > 0$ (the case when $\delta < 0$ is dealt with in the same way).

From the resonance characteristics (23) we can (locally) find $\delta = \delta(a)$ as a function of a and calculate its derivative δ'. It is easy to see[7] that

$$\delta'(a) = \frac{-\tilde{N}'(a)\tilde{N}(a) + (\delta(a))^2 a}{\delta(a)a^2} \tag{24}$$

Therefore we can rewrite the definition (22) of Δ as:

$$\Delta = \frac{-1}{4C^2} a\delta(a)\delta'(a) \tag{25}$$

Consequently the sign of δ' and that of Δ are opposite and $\Delta > 0$ on those parts of the resonance characteristics which decrease when $|\delta|$ grows.

[6]Rigorously speaking we require $N(a)$ to be convex between a_0 and a_2.

[7]Proof follows from the implicit function theorem, also the derivative can be obtained by differentiating (23).

APPENDIX II

A. Averaged Equations

After substitution:

$$v(t) = a\cos(\omega t + \phi)$$
$$i_L(t) = a\frac{\sin(\omega t + \phi)}{\omega L} \tag{26}$$

the circuit equations read:

$$\frac{a'\sin(\omega t + \phi) + a\cos(\omega t + \phi)(\omega + \phi')}{\omega} = a\cos(\omega t + \phi) \tag{27}$$

$$Ca'\cos(\omega t + \phi) - Ca\sin(\omega t + \phi)(\omega + \phi') = -i_L - n(v) - Gv - i_s \tag{28}$$

where $a' = (da/dt), \phi' = (d\phi/dt)$, and $i_s = b\cos\omega t$

The equations simplify to:

$$\begin{bmatrix} \sin\theta & a\cos\theta \\ \cos\theta & -a\sin\theta \end{bmatrix}\begin{bmatrix} a' \\ \phi' \end{bmatrix} = \begin{bmatrix} 0 \\ f \end{bmatrix} \tag{29}$$

where

$$\theta = \omega t + \phi \tag{30}$$

$$f = -\frac{Ga\cos\theta}{C} - \frac{n(a\cos\theta)}{C} + \left(\omega - \frac{1}{\omega LC}\right)a\sin\theta - \frac{b\cos(\omega t)}{C} \tag{31}$$

we solve for a' and ϕ', which results in:

$$a' = f\cos\theta \tag{32}$$

$$\phi' = -\frac{f}{a}\sin\theta \tag{33}$$

After averaging the terms explicitly dependent on time, the circuit equations read:

$$a' = -\frac{Ga + N(a) + b\cos(\phi)}{2C} \tag{34}$$

$$\phi' = -\frac{\delta}{2C} + \frac{b\sin(\phi)}{2Ca} \tag{35}$$

where

$$\delta := C\left(\omega - \frac{1}{\omega LC}\right) = C\frac{\omega^2 - \omega_0^2}{\omega} \approx 2C(\omega - \omega_0) \tag{36}$$

and

$$N(a) = \frac{2}{\pi}\int_0^\pi n(a\cos\theta)\cos\theta\, d\theta \tag{37}$$

B. $N(a)$ for Cubic Nonlinearity

For van der Pol equation we have: $n(v) = -v + (v^3/3)$ consequently:

$$N(a) = -\frac{2}{\pi}\int_0^\pi \left[a\cos\theta - \frac{(a\cos\theta)^3}{3}\right]\cos\theta\, d\theta = -\frac{2}{\pi}\int_0^\pi \left[a\cos\theta^2 - \frac{1}{3}a^3(\cos\theta)^4\right] d\theta = -a\left(1 - \left(\frac{a}{2}\right)^2\right) \tag{38}$$

ACKNOWLEDGMENT

The author thanks to Dr. Tom Parker from Hewlett-Packard Company for many helpful discussions on capabilities of HP Microwave Design System.

REFERENCES

[1] N. N. Bogoliubov and Y. A. Mitropolski, *Asymptotic Methods in the Theory of Nonlinear Oscillations*. New York: Gordon \& Breach, 1961.
[2] J. K. Hale, *Ordinary Differential Equations*. Krieger, 1980.
[3] Ch. Hayashi, *Nonlinear Oscillations in Physical Systems*, New York: McGraw-Hill, 1964.
[4] D. W. Jordan and P. Smith, *Nonlinear Ordinary Differential Equations*. Clarendon, 1977.
[5] K. Kundert and A. Sangiovanni-Vincentelli - "Simulation of nonlinear circuits in the Frequency Domain," *IEEE Trans. Computer-Aided Design*, vol. CAD-5, no. 4, Oct. 1986, pp. 521–535.
[6] K. Kurokawa, *An Introduction to the Theory of Microwave Circuits*. New York: Academic Press, 1969.
[7] K. Kurokawa, "Noise in synchronized oscillators," *IEEE Trans. Microwave Theory Tech.*, vol. 16, pp. 234–240, 1968.
[8] S. A. Maas - *Nonlinear Microwave Circuits*. Norwood, MA: Artech 1988.
[9] M. Odyniec, "Oscillator design using modern CAE," *Electronic Devices and Circuits Forum*, Tokyo, Japan, May 22–23, 1991.
[10] B. van der Pol, "The nonlinear theory of electric oscillators," *Proc. IRE*, vol. 22, no. 9, Sept. 1934.
[11] B. van der Pol, "A theory of the amplitude of free and forced triode vibrations," *Radio Rev.*, vol. 1, 1920.
[12] J. C. Slater, *Microwave Electronics*, Princeton, NJ: Van Nostrand, 1950.

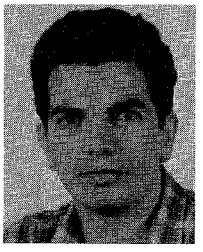

Michal Odyniec received the M.S. in applied mathematics and Ph.D. in electrical engineering both from the Technical University of Warsaw (TUW), Poland.

In 1977 he joined the TUW as an assistant professor, where he worked on nonlinear analysis of circuits and systems, he continued the research when visiting the University of California at Berkeley during the years 1981–1984. In 1985–1989 he worked as a project leader at Microsource Inc. responsible for design of wide band microwave oscillators. In 1989 he joined Hewlettt-Packard's Network and Measurement Division where he works in nonlinear CAE.

Dr. Odyniec is the recipient of Myril B. Reed best paper award. His research interests include nonlinear circuits and systems, microwave and millimeterwave circuits, device modelling and nonlinear dynamics.